

Optimized Surfaces for Second Harmonic Generation from Surface-Plasmon Polaritons: Theory and Experiment

Andrew C.R. Pipino, Richard P. Van Duyne, and George C. Schatz

Department of Chemistry
Northwestern University
2145 Sheridan Road
Evanston, Illinois 60208-3113

ABSTRACT

In connection with recent theoretical predictions, enhancement of optical second harmonic generation (SHG) by diffractive coupling to the silver surface-plasmon polariton (SPP) mode is shown experimentally to be maximized on a biperiodic corrugated surface. Optimized first-order diffractive coupling of incident radiation to the SPP maximizes resonance enhancement of the surface-localized electromagnetic field. Through the nonlinear susceptibility of the silver surface, an SPP-enhanced, evanescent, second harmonic wave is coherently generated which is selectively scattered into the second harmonic specular order by the second spatial harmonic in the surface profile. Biperiodic surfaces with appropriately optimized spatial harmonic composition are shown to provide enhancements in second harmonic reflection of up to 10^4 over the corresponding flat surface response. Using the holographic technique of Breidne et al. (Fourier blaze holography), biperiodic surfaces were fabricated which consisted of a superposition of an 833 nm fundamental and a phase- and amplitude-controlled second spatial harmonic. The results of angle-resolved SHG experiments are presented along with atomic force microscopy (AFM) line scans of the surface profiles. The effect of coupling to the SPP mode at both the incident and second harmonic frequencies is also discussed.

Keywords: surface-plasmon polaritons, second harmonic generation, holography, nonlinear diffraction

1. INTRODUCTION

The study of optical phenomena associated with surface-plasmon polariton coupling has a long and rich history. Existing for metals below the bulk plasma frequency, the SPP is a collective, electronic surface excitation which is manifested as a transverse-magnetic, guided surface wave. To conserve energy and momentum simultaneously in the weak-damping limit, an incident plane wave from vacuum must be scattered by surface roughness to allow interaction with the surface mode. Resonant excitation of the SPP generates large surface fields which are known to enhance spectroscopic observables such as Raman scattering, fluorescence, photochemistry, and SHG. Although many surface-enhanced phenomena have been studied on randomly-rough surfaces, SPP coupling studies on gratings offer the advantage of a well-characterized surface which allows a high-level of experimental control and rigorous theoretical description. In the case of SHG enhancement by SPP coupling on gratings, the coherent nature of the three-photon process gives rise to some unique and potentially useful effects.

In a recent theoretical investigation¹, we examined the influence of coherence and spatial harmonic content on surface-enhanced second harmonic diffraction from silver gratings. In the weak corrugation regime where SPP-coupling efficiency optimizes, it was found that scattering of the SPP-enhanced, evanescent second harmonic wave by spatial harmonics in the surface roughness lead to the selective enhancement of diffraction orders. The SHG intensity in a particular diffraction order could thereby be optimized on a two Fourier component surface by a mechanism which was distinct from the classical blazing effect. The nature of enhancement due to SPP coupling at the second harmonic frequency was also examined. In this work, we demonstrate experimentally the selective enhancement effect for the second harmonic specular order and examine the influence of SPP coupling at the second harmonic frequency. Gratings with varied spatial harmonic composition have been fabricated by using Fourier blaze holography² (FBH), which allows the construction of, in principle, any asymmetric surface profile by superimposing multiple, harmonically-related sinusoids with controlled amplitude and phase. The surface features produced by the Fourier blaze technique are on the order of 10-100 nm in amplitude as required to optimize SPP coupling. To examine the selective enhancement of the second harmonic specular order, the magnitude of the second spatial harmonic has been varied, since this harmonic directly couples the 0-order with the SPP-enhanced, evanescent second harmonic wave¹. It will be shown that surfaces can be fabricated which provide a specular source of SHG in reflection with a gain in intensity of 10^4 over the corresponding flat surface response.

2. EXPERIMENTAL SECTION

2.1 Grating fabrication

The Fourier blaze method allowed the controlled superposition of spatial harmonics in photoresist by use of the Moire pattern generated by an in-plane reference grating. This provided a sensitive probe of the fringe density and phase for harmonically-related interferometric exposures. Two single-mode-stabilized, 457.9 nm, 3" diameter laser beams from an argon-ion laser were interfered on glass substrates (3" x 4") which were spin-coated with 1.5 microns of Shipley 1350B photoresist over an iron oxide layer used to increase resist/substrate adhesion. A maximum of three exposures were carried out for the fabrication of each grating. These correspond to the reference grating, the grating fundamental, and the second harmonic. The central 2" x 2" region of each plate was initially masked off with an opaque developer-tight mask to allow exposure and development of the reference grating on the perimeter of the active area. The reference fringe density of 600 lines/mm, established by using the Moire pattern generated by a *ruled* grating, received a relatively long exposure to create a high diffraction efficiency, 600 groove/mm reference. The photoresist plate position and beam angles were then approximately configured to provide a 1200 line/mm fringe density which was the desired fundamental spatial frequency. The Moire pattern generated by the in-plane reference grating in the vicinity of the 1200 line/mm fringe density was reduced to one or two fringes to eliminate the phase difference between the fringe density and the reference grating to within approximately a tenth of the period. The mask was then removed to allow exposure of the grating fundamental. A fringe-locker³ detected and stabilized the residual Moire pattern thereby locking the phase of the interference fringes relative to the reference grating. After exposure of the 1200 line/mm fundamental, the system was reconfigured for the second spatial harmonic exposure at a 2400 line/mm fringe density. The Moire pattern was again used to establish the correct fringe density

and provide system stabilization. After exposure of the second harmonic, the entire plate was developed in 6:1 diluted 303A developer. The resulting gratings were then coated with 500 nm of high-purity silver by vacuum deposition and stored in a desiccator.

Since the response of the photoresist is nonlinear^{4,5}, a sinusoidal interference pattern did not in general produce a pure sinusoidal grating structure, even for very shallow modulations. As Rosengart and Pockgrand⁶ and Raether⁷ noted, the fabrication of nearly-pure sinusoidal gratings requires the use of a uniform pre-exposure in addition to the interferometric exposure. Pre-exposure of the photoresist allows the most linear region of the exposure versus etch depth curve^{4,5} to be used thereby minimizing the development of unwanted higher harmonics in the surface. To assure that the superimposed exposures contributed nearly-pure, sinusoidal components, an optimal uniform pre-exposure was first determined and then used for all subsequent fabrications. Interferometric exposure times for each harmonic were selected by developing a calibration surface at constant laser power density, which determined groove depth versus exposure and development conditions. The resulting surface profiles were well-described by the function,

$$\zeta(x) = A \left(\sin \frac{2\pi x}{a} + B \sin \frac{4\pi x}{a} \right)$$

where A is the modulation expressed as a small fraction of the period, B is the second harmonic amplitude expressed as a fraction of A, and $a=833.3$ nm. Figure 1 shows AFM line scans for a series of photoresist profiles, where B ranges over $0 \leq B \leq 0.9A$, along with the Fourier transforms. Note that nearly-pure one- or two-Fourier component surfaces are obtained.

2.2 Second harmonic generation measurements

The optical system used for the high-resolution ($\sim 0.01^\circ$) angle-resolved SHG measurements consisted of a Q-switched, Nd:YAG (Quanta Ray DCR-1A) laser operating at 1064 nm with a 10 Hz repetition rate. After filtering the 532 nm radiation arising from a beam reducer and steering optics, the unfocused 2mm diameter, 2-4 mJ/pulse beam was incident on the silver grating. By mounting the grating and a silvered mirror on opposite legs of a 90° reflector which was centered on a high-resolution rotation stage, the incident and reflected beams were always in parallel propagation thereby allowing the angle of incidence to be varied while the collection optics remained fixed. This strategy also allowed the flat silver surface SHG, required for calculating enhancement, to be easily measured under identical alignment conditions. By tuning off of the SPP resonance, the grating served as a mirror which directed the majority of the incident power to the silvered mirror at the complementary angle of incidence. At this angle of incidence, the flat surface SHG was measured with high signal-to-noise ratio and used to obtain the flat surface signal at the actual angle of incidence by comparison with theory^{8,9}, after a small correction for the reflectivity of the grating. The grating-enhanced and flat surface SHG were dispersed by a monochromator and detected by a 1P28 PMT. A reference channel was formed by directing a split-off fraction of the incident pump beam through a quartz wedge followed by several KG5 filters, a monochromator, and a 1P28 PMT. The outputs of the sample and reference PMT's were amplified (x10 Lecroy VV100BTB) and collected by a boxcar averager (PAR) which used a 50 ns aperture duration and was triggered by a reversed-biased photodiode.

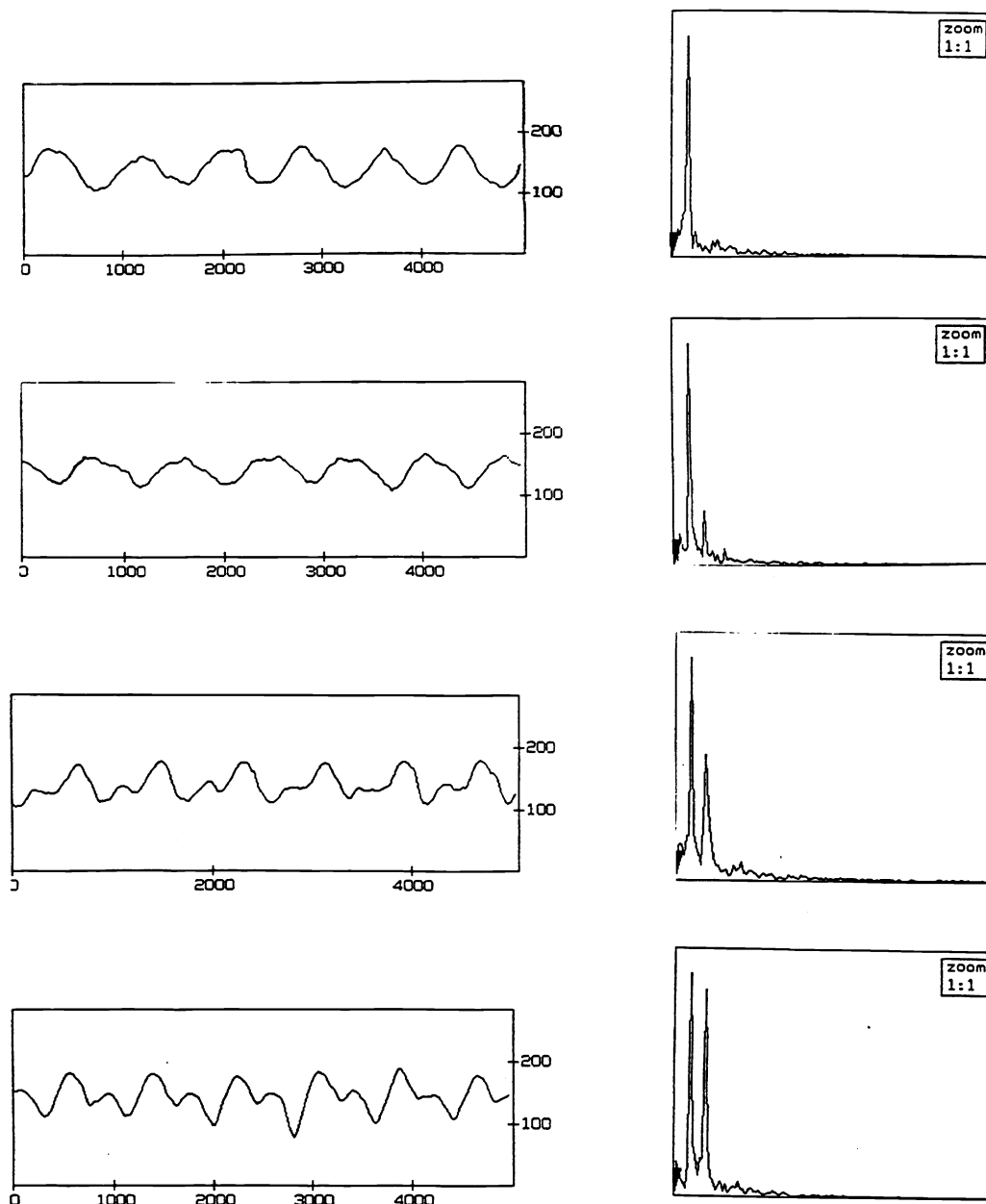


Figure 1. AFM line scans for a series of photoresist profiles produced by the FBH technique. The FFT of the profile trace is shown on the right. The first harmonic for all four profiles was exposed simultaneously, followed by a variable second spatial harmonic exposure. Expressed as a fraction of the fundamental amplitude, the second harmonic amplitudes are approximately: 1a) 0% 1b) 20% 1c) 50% 1d)90%. Note that 1a is a nearly-pure sinusoid and that 1b-1d are well-described as a superposition of two Fourier components. Units are in nanometers.

3. THEORY

The reduced Rayleigh equations, which were first applied to second harmonic diffraction using the source terms of Sipe et al.⁸ by Farias and Maradudin¹⁰, were used. The theory assumes that a p-polarized, plane wave is incident from vacuum onto a corrugated metal surface which is described by the general profile function $z=\zeta(x)$. The dielectric response of the metal is described by bulk dielectric constants $\epsilon(\omega)$ and $\epsilon(2\omega)$. For silver, we use the values of Dujardin and Theye¹¹. The convergence properties of the reduced Rayleigh equations have been discussed elsewhere¹². Enhancement is defined as the ratio of second harmonic diffraction efficiency to the flat surface SHG efficiency at the same angle of incidence.

4. RESULTS AND DISCUSSION

Figure 2a shows calculations which demonstrate the selective enhancement effect. With the amplitude of the fundamental fixed at 8.3 nm (1% modulation), the second harmonic 0-order intensity is seen to vary over several orders of magnitude as the second spatial harmonic amplitude is varied. An optimum amplitude for the second spatial harmonic is also seen to exist. Figure 2b provides an interpretation of this effect using a flat surface SPP coupling diagram. The SPP is efficiently excited in first-order at the pump frequency. Optimization of this coupling and maximization of enhancement of the surface electric field intensity have been discussed elsewhere¹³. Through the second order polarizability of the metal surface, an SPP-enhanced, evanescent second-order wave is generated at $(2k_{sp}, 2\omega)$. Scattering of this evanescent wave into radiative channels largely determines the second harmonic generation properties of the grating in the weak corrugation regime. The second spatial harmonic provides a first-order channel for scattering of the evanescent 2ω wave into the specular order. Figure 3 shows the effect experimentally for a series of gratings with a 1.5% modulation fundamental. Note that even though these enhancements are defined relative to the flat surface response at the same angle of incidence, the efficiency of second harmonic conversion still exceeds that from randomly-rough surfaces¹⁴.

Figure 4 shows experimentally the effect of SPP coupling at the SH frequency. By varying the period for a series of nearly-pure sinusoidal gratings, the condition in which both the incoming ω pump beam and the outgoing 2ω 0-order diffracted beam differ from SPP resonances (at ω and 2ω , respectively) by a single grating wavevector, is probed. Since enhancement is defined relative to the flat surface response which increases rapidly with increasing angle of incidence, the enhancement for a series of profiles with fixed depth and decreasing period would be expected to decrease rapidly due to the increasing SPP coupling angle. Instead, a maximum is observed for a period of 773.8 nm. The modulation for this series of profiles is approximately 2%. For a 4% modulation the effect is predicted to be far more pronounced¹.

5. CONCLUSIONS

A strong dependence of SPP-enhancement of SH diffraction on surface spatial harmonic content has been shown for silver. Large enhancements can be obtained when scattering of the SPP-enhanced, evanescent 2ω wave is optimized in addition to optimization of SPP coupling. The coherent nature of SHG allows both processes to be optimized on a biperiodic corrugated surface.

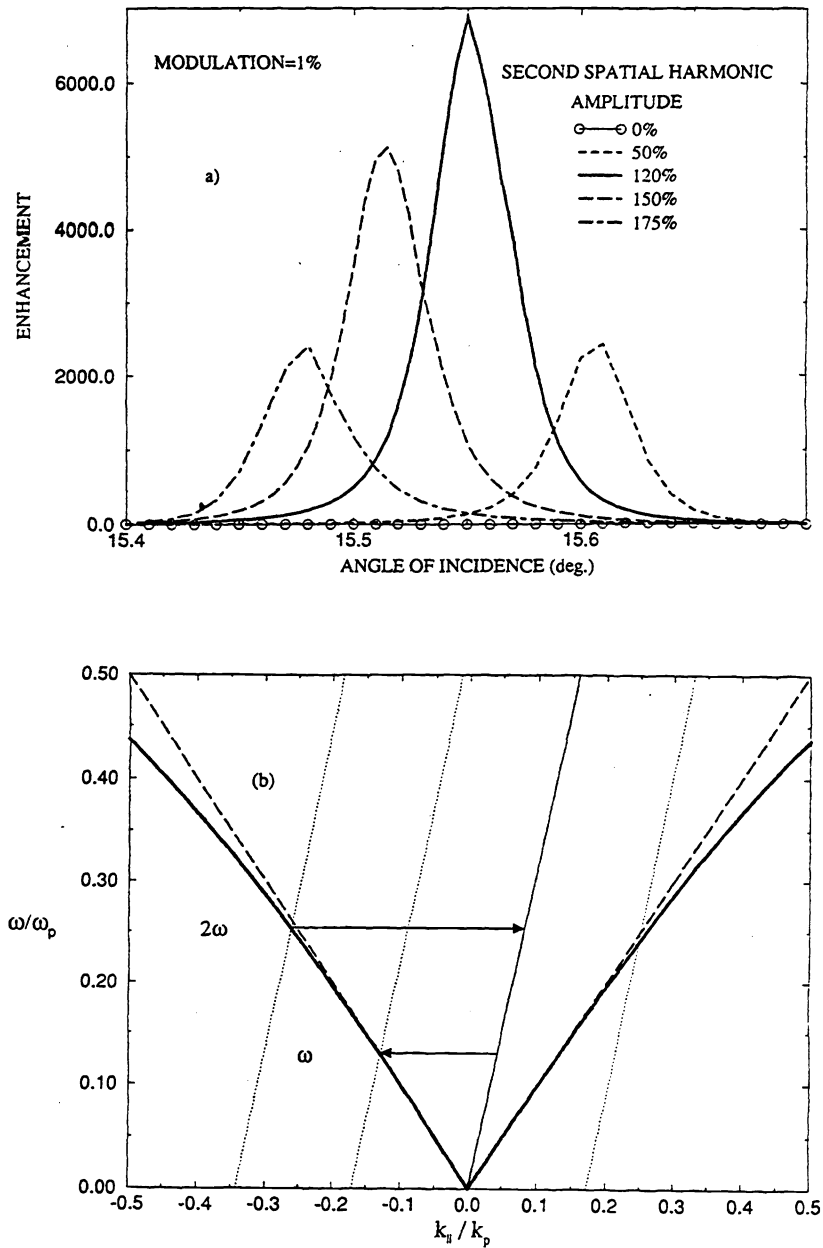


Figure 2. a) Theoretical predictions showing enhancement of second harmonic reflection by the phase- and amplitude-controlled addition of second spatial harmonic to the surface profile. An optimum value of ~ 10 nm for the second harmonic amplitude is predicted. The pure sinusoidal case shows negligible enhancement on this scale. b) Interpretation of the effect using the flat surface SPP dispersion relation.

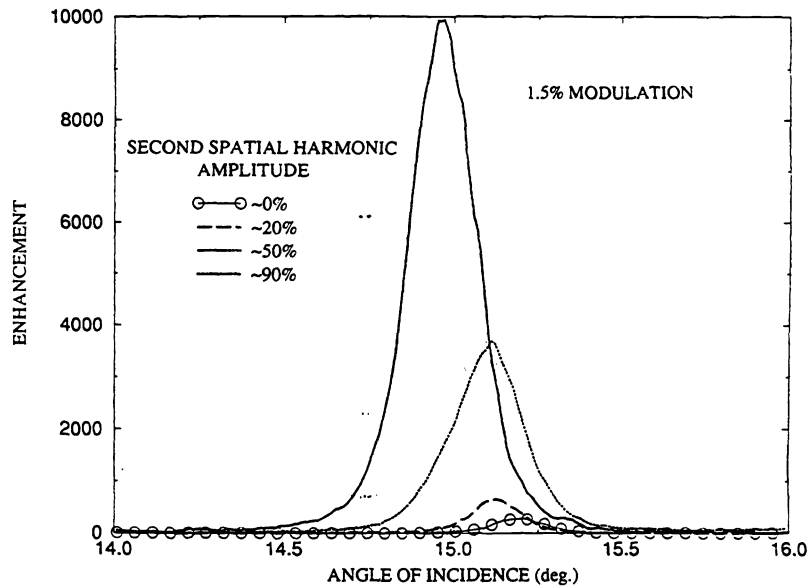


Figure 3. Angle-resolved SHG measurements for the metalized profiles of Figure 1, showing the predicted strong dependence of second harmonic reflection on the second spatial harmonic in the surface profile. Note that the FWHM of these peaks remains essentially constant as the second harmonic amplitude is varied, as expected for approximately uncoupled scattering processes at ω and 2ω .

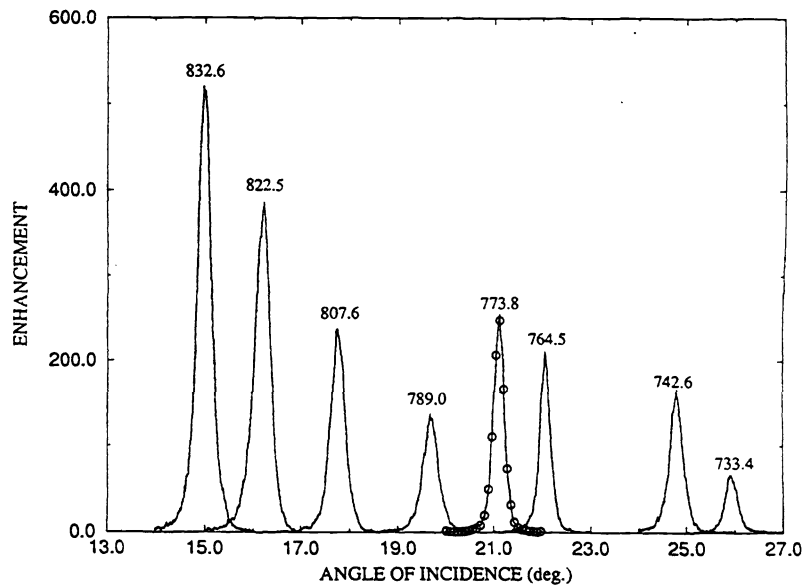


Figure 4. Angle-resolved SHG measurements for a series of nearly-pure sinusoidal gratings with different periods, which allows "tuning" through the $\omega/2\omega$ double SPP resonance.

6. ACKNOWLEDGEMENTS

The authors gratefully acknowledge Tom O'Connor and Steve Smith of Lasersmith Inc. for technical assistance with the grating fabrication. We would also like to thank Prof. Rob Corn and Group at UW, Madison for advice concerning SHG measurements. This work was supported in part by the Donors of the Petroleum Research Fund of the American Chemical Society (Grant No. 29507-AC6) and in part by NSF Grant Nos. DMR-8802706, CHE-940078, and CHE-9016490.

7. REFERENCES

- 1) A.C.R. Pipino, G.C. Schatz, and R.P. Van Duyne, "*Surface-enhanced second harmonic diffraction: Selective enhancement by spatial harmonics*" Phys. Rev. B **49**, 8320 (1994).
- 2) M. Breidne, S. Johansson, L-E. Nilsson, and H. Åhlén, "*Blazed holographic gratings*", Optica Acta **26**, 1427 (1979).
- 3) D.R. MacQuigg, "*Hologram fringe stabilization method*", Appl. Opt. **16**, 291 (1977).
- 4) S. Austin and F.T. Stone, "*Fabrication of thin periodic structures in photoresist: a model*", Applied Optics **15**, 1071 (1976).
- 5) S. Austin and F.T. Stone, "*Thin periodic structures in photoresist: fabrication and experimental evaluation*", Applied Optics **15**, 2126 (1976).
- 6) E.-H. Rosengart and I. Pockrand, "*Influence of higher harmonics of a grating on the intensity profile of the diffraction orders via surface plasmons*", Optics letters **1**, 194 (1977).
- 7) H. Raether, "*Dispersion relation of surface plasmons on gold- and silver gratings*", Opt. Commun. **42**, 217 (1982).
- 8) J.E. Sipe, V.C.Y. So, M. Fukui, and G.I. Stegeman, "*Analysis of second harmonic generation from metal surfaces*", Phys. Rev. B **21**, 4389 (1980).
- 9) J.C. Quail and H.J. Simon, "*Second harmonic generation from a silver grating with surface plasmons*", J. Opt. Soc. Am. **5**, 325 (1988).
- 10) G.A. Farias and A.A. Maradudin, "*Second-harmonic generation in reflection from a metallic grating*", Phys. Rev. B **30**, 3002 (1984).
- 11) M.M. Dujardin and M.L. Theye, "*Investigation of the optical properties of Ag by means of thin semi-transparent films*", J. Phys. Chem. Solids **32**, 2033 (1971).
- 12) T.C. Paulick, "*Applicability of the Rayleigh hypothesis to real materials*", Phys. Rev. B **42**, 2801 (1990).
- 13) N. Garcia, G. Diaz, J.J. Saenz and C. Ocal, "*Intensities and field enhancement of light scattered from periodic gratings: Study of Ag, Au, and Cu surfaces*", Surf. Sci. **143**, 342 (1984).
- 14) G.T. Boyd, Th. Rasing, J.R.R. Leite, Y.R. Shen, "*Local-field enhancement on rough surfaces of metals, semimetals, and semiconductors with the use of optical second harmonic generation*", Phys. Rev. B **30**, 519 (1984).